Reports

High-Latitude Stratospheric Aerosols Measured by the SAM II Satellite System in 1978 and 1979

Abstract. *Results of the first year of data collection by the SAM (Stratospheric Aerosol Measurement) II satellite system are presented. Almost 10,000 profiles of stratospheric aerosol extinction in the Arctic and Antarctic regions are used to construct plots of weekly averaged aerosol extinction versus altitude and time and stratospheric optical depth versus time. Corresponding temperature fields are presented. These data show striking similarities in the aerosol behavior for corresponding seasons. Wintertime polar stratospheric clouds that are strongly correlated with temperature are documented. They are much more prevalent in the Antarctic stratosphere during the cold austral winter and increase the stratospheric optical depths by as much as an order of magnitude for a period of about 2 months. These clouds might represent a sink for stratospheric water vapor and must be considered in the radiative budget for this region and time.*

The stratospheric aerosol layer composed of submicrometer-sized particles is found in the lower to middle stratosphere. In this layer the mixing ratio of large particles (radius > 0.15 μm) reaches a maximum of about 10 particles per milligram of air in nonvolcanic periods at about 10 km above the local tropopause (*1*). Likewise, peak concentrations for these particles of about 0.5 cm^{-3} occur at about 6 km above the local tropopause. These values drop off quickly at altitudes between 25 to 30 km. The exact composition of the aerosol is uncertain, but most evidence indicates that it is a 75 percent (by mass) solution of sulfuric acid with water (*2*). The primary source of sulfur is thought to be tropospheric OCS (*3*). The properties of stratospheric aerosols are reviewed by Toon and Farlow (*4*). This aerosol layer is thought to exert an influence on the earth's climate (*5, 6*), and consequently has been the subject of various measurement programs designed to quantify characteristics such as its geographic and seasonal variations or to determine properties of the aerosol particles themselves, such as composition and size distribution.

Recently, NASA launched two satellites bearing instruments designed to monitor the stratospheric aerosol layer (*7*). These instruments are referred to by the acronyms SAM II (Stratospheric Aerosol Measurement II) and SAGE (Stratospheric Aerosol and Gas Experiment). The SAM II system is designed to measure the spatial distribution of aerosols at high latitudes; SAGE, launched 4 months after SAM II, measures aerosol and ozone primarily at tropical and midlatitudes.

In this report we present, in a highly condensed form, results obtained from the first 12 months of the SAM II operations. The data reveal interesting seasonal similarities between the two polar regions. In addition, strong correlations with the averaged temperature fields are apparent.

The SAM II experiment determines vertical profiles of atmospheric aerosol extinction by measuring the attenuation of 1-μm wavelength solar radiation that has passed through the earth's atmosphere before reaching the satellite detector (*8*). Integrating the extinction profiles from the tropopause through the stratosphere yields stratospheric aerosol optical depth. Both extinction and optical depth data are presented in this report.

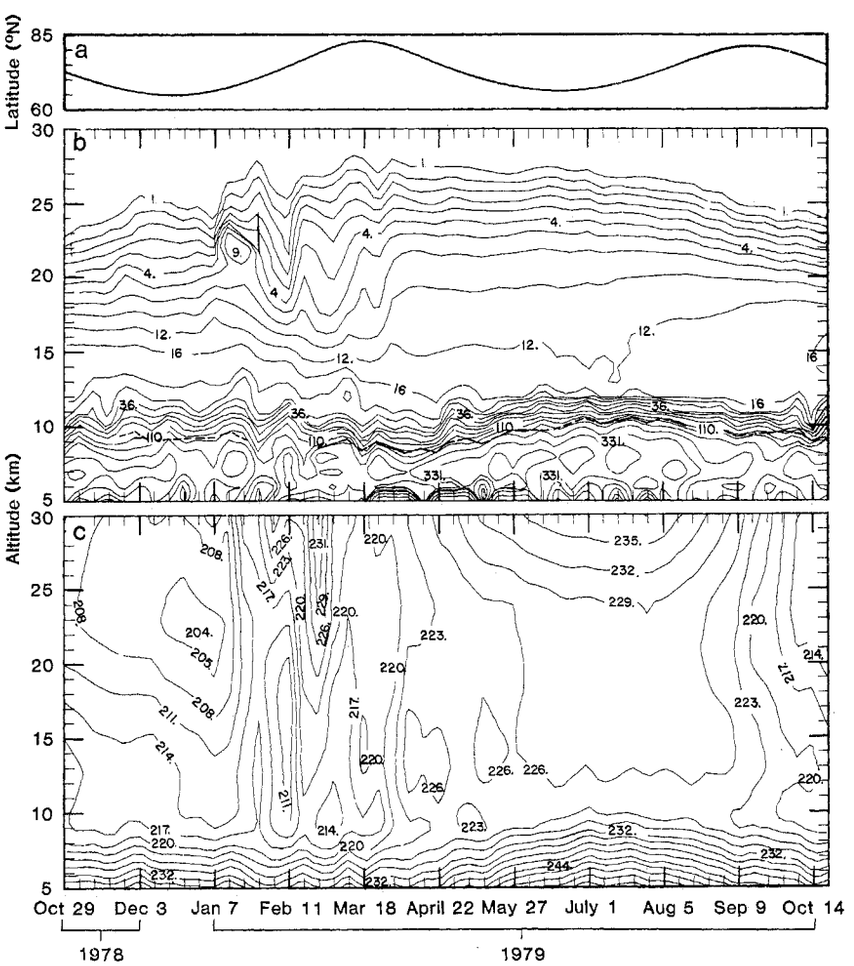

Fig. 1. Northern Hemisphere weekly averaged values; the date marked on the horizontal axis is the first day of the week to which the average value corresponds. (a) Latitude of measurement. (b) Aerosol extinction at 1 μm in units of 10^{-5} km^{-1}; the interval between adjacent isopleths is a multiple of ~ 1.32. Darker dashed line around 10 km indicates tropopause height. (c) Temperature field in kelvins at the location of the aerosol measurement; the isotherms are separated by 3 K.

0036-8075/81/1016-0328$01.00/0

Sampling opportunities occur twice per orbit during each sunrise and sunset encountered by the satellite. Due to the orbital characteristics of the Nimbus-7 satellite on which the SAM II instrument is mounted, the sunrises occur in the Southern Hemisphere between 64° and 81°S and the sunsets occur in the Northern Hemisphere between 65° and 82°N. The orbital period of Nimbus-7 is 104 minutes, so approximately 14 sunrises and 14 sunsets are encountered daily. Consecutive profiles are separated by 26° in longitude but are at nearly the same latitude. The latitudinal variation of the sampling tangent point for each profile is only 2° or less per week. These satellite measurements vary from one extreme in latitude to the other in about 13 weeks; hence, there are four such sweeps per year, as shown in Figs. 1a and 2a. The minimum and maximum latitudes occur at the solstices and equinoxes, respectively. Results obtained with SAM II have been compared with ground-truth (or correlative) measurements made at the same time and place by other instruments (particle counters and a laser radar). The SAM II results agree well with the correlative measurements within an extinction error of approximately 10^{-5} km^{-1} (*9*).

Figures 1b and 2b show isopleths of aerosol extinction as a function of altitude and time for the Arctic and Antarctic regions in Figs. 1a and 2a, respectively. Each tick mark on the horizontal axes indicates the input of a single profile obtained by averaging the 97 profiles for that week. The dashed, nearly horizontal lines near altitude 10 km show the position of the tropopause; breaks in these lines indicate that tropopause data were not available. Figure 1b gives the extinction in the Northern Hemisphere for 29 October 1978 through 27 October 1979. Figure 2b displays the equivalent information for the Southern Hemisphere, but displaced by 26 weeks to facilitate a comparison of seasonal behavior in the two hemispheres. As shown in Figs. 1a and 2a, the latitude band is narrow (17°) and is covered fully in each season. Thus, although variations in extinction may be ascribed to the latitudinal progression, they are probably more indicative of seasonal changes in the aerosol in the latitude band as a whole. Figures 1c and 2c show the pertinent weekly averaged temperature data. Temperature profiles were supplied by the U.S. National Weather Service and correspond to the location and time of the SAM II profiles.

Many similarities in the behavior of the stratospheric aerosol in the two polar regions are apparent. Note, for example, the increased extinction found at various altitudes in both hemispheres in the winter period. We analyzed these increases in extinction and concluded that they are manifestations of polar stratospheric clouds, probably composed of a highly diluted sulfuric acid aerosol in the liquid or solid (ice) phase (*10*). Stratospheric clouds formed during the Arctic winter season cause high extinctions in the altitude range 20 to 25 km. The length and severity of the Antarctic winter, with temperatures as low as 187 K (about 17 K lower than the coldest Arctic temperatures for this year), resulted in extinctions as much as an order of magnitude greater than the corresponding Arctic values (see Fig. 2b, June to September 1979). Toward the end of the Antarctic winter the aerosol layer descended, bringing the height of the top of the layer (as defined by the 1.0×10^{-5} km^{-1} isopleth, the uppermost curve on our graphs) down to about 18 km. This descent preceded a dramatic stratospheric warming, which was most rapid at these heights during the spring equinox. Previous studies showed the subsidence of stratospheric air that accompanies the development of sudden warmings and documented similar effects on both ozone and aerosol layers (*11*). After the warming the top of the layer rose suddenly to a height of about 27 km. It is not clear whether the aerosol apparent between 18 and 27 km following the warming is due to lifting of the depressed layer or to growth or injection of new aerosols in this region.

The Arctic aerosol exhibited similar behavior in midwinter; that is, the layer tended to dip down and then rise as the stratosphere warmed, but the relative mildness of the winter and the warming led to less dramatic transitions in the aerosol layer (*12*). The polar stratospheric clouds in the Arctic (indicated by increased extinction at about 22 km in early January) disappeared as tempera-

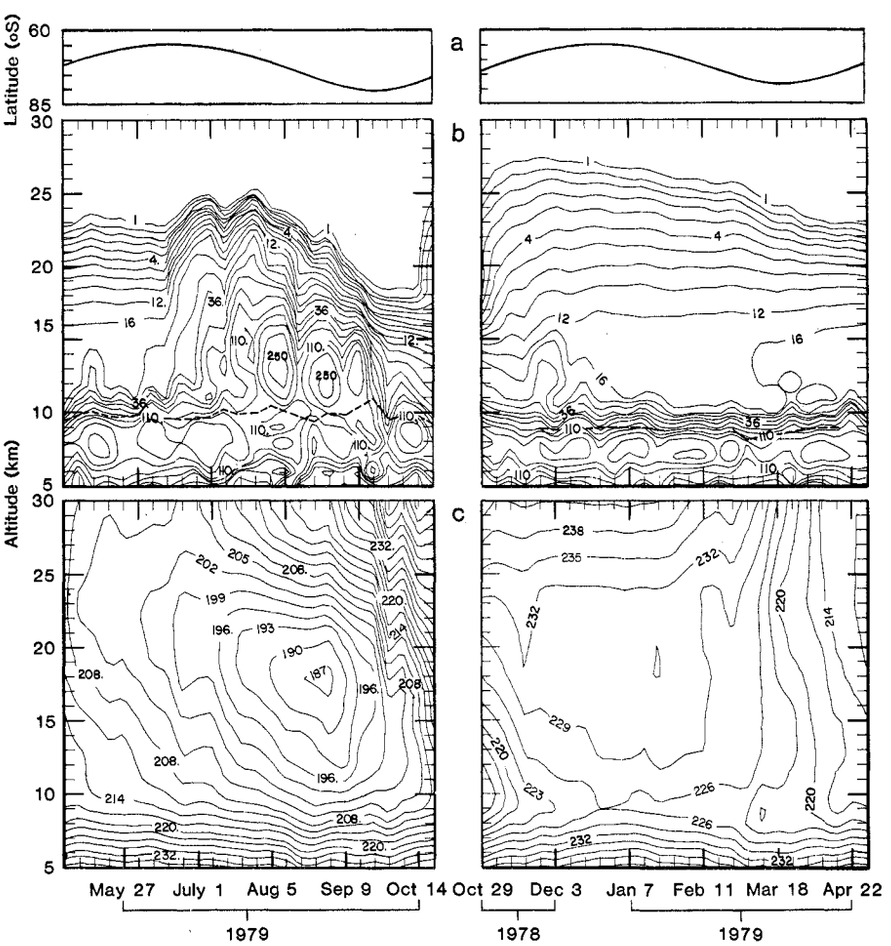

Fig. 2. Southern Hemisphere weekly averaged values; the date marked on the horizontal axis is the first day of the week to which the average value corresponds. (a) Latitude of measurement. (b) Aerosol extinction at 1 μm in units of 10^{-5} km^{-1}; the interval between adjacent isopleths is a multiple of ~ 1.32. Darker dashed line around 10 km indicates tropopause height. (c) Temperature field in kelvins at the location of the aerosol measurement; the isotherms are separated by 3 K. This figure covers the same time interval as Fig. 1 but was divided into two halves which were interchanged so that the same seasons in the two figures are aligned.

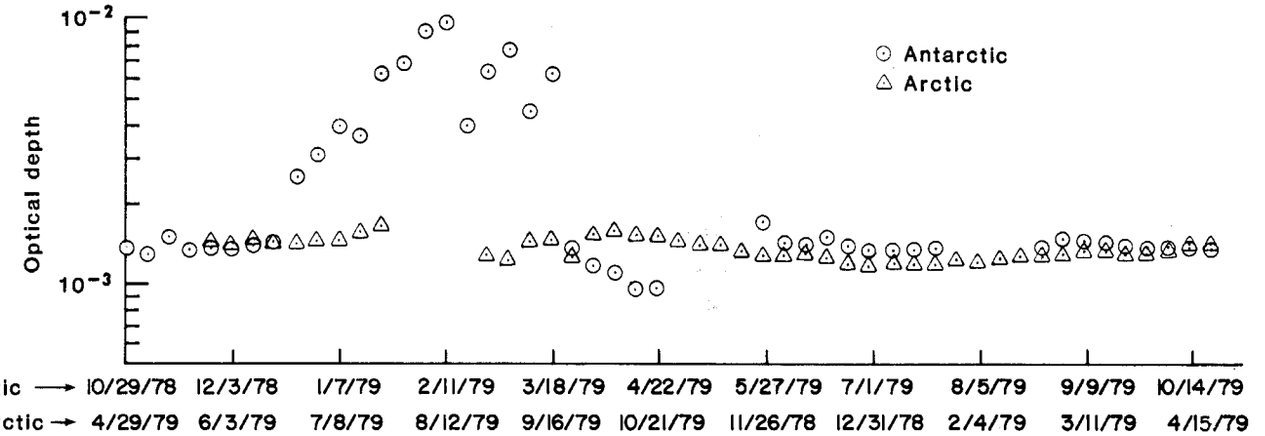

Fig. 3. Weekly averaged optical depths from the tropopause plus 2 km to 30 km for the Southern and Northern hemispheres for wavelength 1 μm. Note that the Antarctic values are displaced by 6 months. Some values are missing where tropopause height was not available.

tures rose between mid-January and early February. The Antarctic clouds similarly disappeared during the week beginning 23 September as a rapid warming occurred.

After this period in both hemispheres the top of the aerosol layer reached its maximum altitude in the spring and then fell slowly and steadily through the summer, staying fairly constant at about 23 to 25 km during most of the fall as the stratosphere cooled. Another insight into the vertical extent of the layer can be gained by noting the separation of two contours—for example, those marked 4 and 16. This separation was at its greatest during the late spring to early summer, indicating a broad aerosol layer, and reached its minimum during the fall and winter period.

The contour level 16×10^{-5} km^{-1} is interesting to follow by itself. This isopleth fell in altitude throughout the middle to late winter and spring, reaching its lowest height at about the time of the summer solstice. It remained just above the tropopause throughout the summer months, when the temperature in both hemispheres at this altitude remained fairly constant at about 226 K. A doubling back of this contour indicating a peak in the extinction profile of about 16×10^{-5} km^{-1} appears in both polar regions near the beginning of fall, as the stratosphere becomes cooler and more isothermal. The occurrence of such similar behavior in the two hemispheres is striking.

The corresponding 1-year optical depth data set is shown in Fig. 3. The optical depths were obtained by integrating each aerosol extinction profile from 2 km above the tropopause to 30 km and calculating an average value for each week. Except for the Antarctic winter period, the optical depth in the two hemispheres is similar. In the Antarctic winter the onset of polar stratospheric clouds caused a sudden and persistent increase in optical depth, with values as much as an order of magnitude higher than those for the rest of the year. A small increase in the Arctic optical depth during the beginning of the winter season was also observed. The disappearance of the Antarctic stratospheric clouds corresponding to the rapid spring increase in temperature is evident in the optical depth data.

The values of polar stratospheric aerosol optical depth at 1.0 μm given in Fig. 3 provide the most comprehensive data set of this type available and should be valuable for optical models of this atmospheric region. In addition, the winter Antarctic values greater than 5×10^{-3} for approximately 7 weeks and 3×10^{-3} for 10 weeks represent a radiative perturbation to this part of the globe with possible surface and stratospheric temperature effects. Furthermore, this long-term cloud formation could result in loss of stratospheric water vapor and aerosols if the cloud particles are removed by sedimentation or other processes. It is interesting to note that the stratospheric optical depth does fall to its lowest value in the Antarctic spring.

A much more extensive analysis of the results of the SAM II experiment and compilations of extended data sets and results will be made available in a series of NASA reports (*13*). The raw data, inverted extinction profiles, maps, and matrices will be archived on magnetic tape and microfilm at the National Space Sciences Data Center (*14*), where they will be available for use by interested scientists. The results in Figs. 1 to 3 are, to our knowledge, the most complete representation to date of the high-latitude stratospheric aerosol. Almost 10,000 individual profiles were used to construct these plots, so the values given should not be influenced by small-scale time and space variations in the layer. Except for the stratospheric cloud perturbations in winter, we feel that these results can be classified as background values, although the clouds may turn out to be representative of local winter conditions. The last volcanic eruption to inject a significant amount of material into the stratosphere was that of Volcán de Fuego in Guatemala in 1974 (*15*). The *e*-folding residence time for volcanic residue from Fuego in the stratosphere was less than 1 year (*16, 17*). Therefore, there is reason to believe that the extinction values reported here are representative of a nonvolcanic background aerosol.

M. P. McCormick
W. P. Chu
NASA Langley Research Center, Hampton, Virginia 23665
G. W. Grams
School of Geophysical Sciences, Georgia Institute of Technology, Atlanta 30315
Patrick Hamill
Systems and Applied Sciences Corporation, Hampton, Virginia 23666
B. M. Herman
Institute of Atmospheric Physics, University of Arizona, Tucson 85721
L. R. McMaster
NASA Langley Research Center
T. J. Pepin
Department of Physics and Astronomy, University of Wyoming, Laramie 82071
P. B. Russell
SRI International Menlo Park, California 94025
H. M. Steele
T. J. Swissler
Systems and Applied Sciences Corporation

References and Notes

1. J. M. Rosen and D. J. Hofmann, *J. Atmos. Sci.* **32**, 1457 (1975).
2. J. M. Rosen, *J. Appl. Meteorol.* **10**, 1044 (1971).
3. P. J. Crutzen, *Geophys. Res. Lett.* **3**, 73 (1976).
4. O. B. Toon and N. W. Farlow, *Annu. Rev. Earth Planet. Sci.* **9**, 19 (1981).
5. J. B. Pollack, O. B. Toon, C. Sagan, A. Summers, B. Baldwin, W. Van Camp, *J. Geophys. Res.* **81**, 1071 (1976).
6. J. B. Pollack, A. Summers, B. Baldwin, C. Sagan, W. Van Camp, *Nature (London)* **263**, 551 (1976).
7. For a complete description of the SAM II and SAGE systems, see M. P. McCormick, P. Hamill, T. J. Pepin, W. P. Chu, T. J. Swissler, L. R. McMaster, *Bull. Am. Meteorol. Soc.* **60**, 1038 (1979).
8. The inversion techniques used are discussed in W. P. Chu and M. P. McCormick, *Appl. Opt.* **18**, 1404 (1979).
9. P. B. Russell *et al.*, *J. Atmos. Sci.* **38**, 1295 (1981).
10. J. L. Stanford and J. S. Davis, *Bull. Am. Meteorol. Soc.* **55**, 213 (1974); M. P. McCormick, H. M. Steele, P. Hamill, W. P. Chu, T. J. Swissler, in preparation; P. Hamill, H. M. Steele, M. P. McCormick, W. P. Chu, T. J. Swissler, in preparation.
11. A. Ghazi, *J. Atmos. Sci.* **31**, 2197 (1974); P. B. Russell, W. Viezee, R. D. Hake, R. T. H. Collis, *Q. J. R. Meteorol. Soc.* **102**, 675 (1976).
12. For details of this stratospheric warming, see R. S. Quiroz, *Geophys. Res. Lett.* **6**, 645 (1979).
13. M. P. McCormick, H. M. Steele, P. Hamill, T. J. Swissler, W. P. Chu, L. R. McMaster, W. H. Mitchell, A. B. Graham, M. T. Osborn, *NASA Ref. Publ. L-14754*, in press.
14. National Space Sciences Data Center, NASA Goddard Space Flight Center, Greenbelt, Md. 20771.
15. The eruption of Soufrière on the Caribbean island of St. Vincent in April 1979 did not inject a significant amount of material into the stratosphere. It represented about a 0.5 percent increase in stratospheric aerosol mass.
16. M. P. McCormick, T. J. Swissler, W. P. Chu, W. H. Fuller, *J. Atmos. Sci.* **35**, 1296 (1978).
17. D. J. Hofmann and J. M. Rosen, *ibid.* **38**, 168 (1981).

24 March 1981; revised 16 July 1981

Superheavy Elements: An Early Solar System Upper Limit for Elements 107 to 110

Abstract. *The abundance of samarium-152 in the Santa Clara iron meteorite is found to be 108 × 10^7 atoms per gram. This quantity, if attributed to fission of a superheavy element with atomic number 107 to 109, limits the amount of superheavy elements in the early solar system to 1.7 × 10^{-5} times the abundance of uranium-238. For element 110, the limit is 3.4 × 10^{-5}*

Superheavy elements (SHE's) are elements with atomic numbers greater than 106 which may have been produced in stars by the same processes that produced thorium, uranium, and plutonium. Myers and Swiatecki (*1*) suggested that a region of relative stability, which would permit some of these elements to have appreciable half-lives, existed near atomic number $Z = 114$ and neutron number $N = 184$. More recent calculations, in which alpha and beta decay were considered in addition to spontaneous fission, suggest that the most stable nuclide is $^{294}110$, with a half-life ($t_{1/2}$) of 10^5 to 10^9 years (*2*). Numerous attempts have been made to synthesize SHE's in the laboratory and to search for them in nature. The possibility of an SHE with $t_{1/2} \approx 10^9$ years has led many investigators to search for extant SHE's; claims have been made for their discovery in halos in mica (*3*), in meteorites (*4*), and in hot springs (*5*), but these claims have been criticized (*6*). Other investigations are discussed in several reviews (*7*); there is currently no strong evidence for extant SHE's. Anders and co-workers (*8, 9*) claimed evidence for an extinct SHE with $Z = 115$ (or 114 or 113) in the Allende meteorite, based on xenon isotopic abundances that appear to be due to fission of an unknown transuranic nuclide. This result is difficult to understand in terms of calculated half-lives for these nuclides, all of which are less than 1 year, based on the more recent calculations (*2*). However, the calculated half-lives are uncertain by many factors of 10 (*10*).

We designed an experiment to look specifically at element 110, the only one expected to have a half-life long enough to have survived until the formation of the solar system. We chose an iron meteorite, Santa Clara, for our study because elements 107 through 110 are expected to be siderophilic, that is, concentrated in metallic phases, whereas the rare earth fission decay products are not. Santa Clara was chosen because it contains evidence for decay of extinct ^{107}Pd ($t_{1/2} = 6.5 \times 10^6$ years) (*11*). Because this meteorite apparently formed very early after nucleosynthesis, it may contain evidence for SHE's with half-lives as short as a few million years. In order to explain the applicability of meteorites in addressing this problem, we will describe the mechanism by which iron meteorites are thought to have formed.

Initially, solid grains of metals and silicates condensed out of a hot solar nebula. These grains accreted to form larger bodies that eventually melted. The metal grains sank and coalesced to form an iron-nickel core with a silicate mantle. Later collisions with other bodies fragmented the object. A sample of this core was eventually perturbed into an earth-crossing orbit, and fell as a meteorite.

By considering the thermodynamic properties of the elements, one can calculate the fraction of an element condensed into the grains as a function of temperature. Santa Clara is a typical member of the group IVB irons, which, on the basis of several elements, give a self-consistent grain condensation temperature of 1270 K at a pressure of 10^{-5} atm (*12*). At this temperature Fe and Ni are about 10 percent condensed, while Re, Os, Ir, and Pt, congeners of SHE's 107 to 110, are totally condensed. This work is mainly aimed at SHE 110, the only element expected to have a long half-life, but because the calculated half-lives for fission are so uncertain, elements 107 to 109 are also considered.

To consider the properties of the SHE's in detail and to calculate the fraction condensed, we require estimates of their enthalpy (ΔH_v) and entropy (ΔS_v) of vaporization. Following other investigators (*8, 13*), we extrapolate values from congeners in other rows of the periodic table. The values of ΔH_v are plotted in Fig. 1 (*14*). The extrapolation for elements 107 to 109 appears straightforward, with a clear monotonic trend toward increasing ΔH_v with increasing period. For element 110 the extrapolation is less certain. We arbitrarily chose a value as indicated, but any value from 100 to about 180 kcal is plausible. For comparison, the value chosen by Anders *et al.* (*8*) for element 111 in a similar situation is indicated. Following the procedures of Kelly and Larimer (*12*), we calculated the fraction of each SHE condensed at 1270 K and 10^{-5} atm. Even the most volatile element, element 110, is 99.98 percent condensed under these conditions. Deviations from ideal solid solution, if similar to Pt in Ni (*15*), would increase the amount of element 110 condensed. Because the extrapolation of ΔH_v for element 110 is uncertain, we will be conservative and assume that it is only 50 percent condensed; this is the observed fraction condensed of Pd, the most volatile congener of element 110 (*16*).

Abundances of the rare earth elements were determined by neutron activation analysis with radiochemical separation (*17*). The results are given in Table 1. Neutron activation analysis can only determine the quantity of the target nuclide; except for monoisotopic elements, the technique generally does not directly determine the total amount of the element present. The assumption of normal isotopic abundance to infer the total quantity of an element may not be appropriate in this instance, since significant

0036-8075/81/1016-0331$01.00/0